Validation of Triton Wind Profiler Measurements in Complex Terrain, Using WindSim CFD-Based Flow Curvature Correction

February 2018
Dr. Mark Stoelinga, Senior Scientist
Niels LaWhite, Senior Scientist

Executive Summary

Vaisala and WindSim have developed a computational fluid dynamics (CFD) model–based correction to flow curvature bias incurred by remote sensing devices when used in complex terrain. CFD model–based corrections are helping to pave the way for greater reliance on remote sensing–based wind speed measurements for sites affected by complex wind flow. This paper describes our method for correcting wind speed measurements and shows the results of a study to validate measurements corrected with this method against collocated met towers. This work represents a follow-up to our 2015 validation study of Triton Wind Profilers in mostly flat terrain.

We compiled a validation dataset comprising measurements from 26 Tritons collocated with met towers at project development sites across the globe in varying degrees of terrain complexity, in order to obtain robust guidance on Triton uncertainty in real-world deployments. We found that the CFD-based corrections are able to substantially remove the flow curvature bias. Application of the CFD correction factors reduced the dataset-wide difference in mean wind speed measured by Triton and met towers from −2.4% to −0.1%. In other words, the bias across the entire dataset was removed by the CFD-based corrections. The standard deviation of the differences between Triton and met tower mean wind speeds across all the met towers was reduced from 3.2% to 2.3%. The equivalent metric in the flat-terrain study was 1.3%. By performing multiple experiments with and without corrections applied, we were able to isolate the uncertainty of the Triton measurement with respect to true wind speed (rather than with respect to the nearby met tower) that remained after the flow curvature correction was applied, which is of greatest interest for wind resource assessment. This uncertainty was 2.0%, compared to an analogous estimate in the flat terrain study of 1.0%. Finally, we developed an ensemble of flow curvature bias estimates by perturbing the calculation method, and found the ensemble spread to be a good predictor of site-specific uncertainty of the corrected Triton measurements with respect to true wind speed. Using this approach, we found that the uncertainty of Triton mean wind speed with respect to true mean wind speed spanned a range from 1.2% at the least uncertain validation point, to 3.3% at the most uncertain validation point, with a median uncertainty of 1.9%. The uncertainty also tended to decrease with measurement height, which was an encouraging result considering the ever-increasing heights of modern wind turbines.

1 Motivation

As the wind industry expands to more diverse and challenging locations across the globe, wind measurement campaigns (whether for resource assessment or operational monitoring) require measurement technology that is cost-effective, rapidly deployable to remote locations, and reliably accurate at the hub heights of modern utility-scale wind turbines, in all types of terrain and land surface.

The Vaisala Triton Wind Profiler is one such technology. It is a sodar-based device for obtaining measurements of wind speed and direction in the lowest 200 m of the atmosphere, and has been deployed at thousands of diverse locations across the globe in support of wind energy development and operations. Vaisala conducted a comparison study of 30 globally distributed Tritons with collocated met towers in mostly flat terrain [1], hereinafter referred to as the "flat-terrain study", and found that the overall mean wind speed difference was unbiased, and the distribution of mean wind speed differences yielded a root mean-squared (RMS) value of 1.3%. From these results, Vaisala concluded that Triton exhibited an uncertainty with respect to true mean wind speed of around 1%.

Most remote sensing devices (RSD), including Triton, use Doppler-based measurement with a divergent beam configuration, and therefore rely on an assumption of horizontal uniformity of flow, because the beams are sampling horizontally separated locations at a given height, but treating them as the same location. Over complex terrain, however, wind flow can exhibit significant curvature, which violates the assumption of flow uniformity, and leads to flow curvature bias in the measurement. Several studies have shown that this measurement bias can be reduced by simulating the airflow over the site with wind flow modeling, deriving correction factors from the model output, and applying those correction factors to the measurements (see [2], and references therein). Vaisala is partnering with WindSim, a leader of CFD modeling in the wind industry, to provide a CFD model simulation and flow curvature correction capability, now available to Triton users. The model uses a standardized configuration that can be set up and executed rapidly, anywhere across the globe. This ease of application, in conjunction with the availability of a large number of Tritons deployed in complex terrain with collocated met towers, gives us the opportunity to test the methodology across a large set of Triton/met tower pairs.

As with the flat-terrain validation study, this study goes beyond demonstrating that the technology works for one Triton in an idealized experiment. Because we use actual customer data at many diverse sites, the results of this study reflect the accuracy that Triton users can expect when they deploy their device in real-world measurement campaigns and apply Vaisala/WindSim's flow curvature correction to their data. This study will provide guidance on the uncertainty of Triton measurements in complex terrain using flow curvature correction, as a companion to the guidance on uncertainty of Triton measurements in flat terrain already provided in the 2015 study [1].

2 Flow Curvature Correction

2.1 *The phenonomenon of flow curvature bias*

The effect of complex terrain and associated flow curvature on measurements from a divergent–beam Doppler-based RSD can be understood by considering the difference between flow over flat terrain versus a hill, as depicted in Fig. 1. The blue features represent flow over flat terrain, whereas the orange features represent curved flow over convex terrain (a hill top). In the divergent beam configuration, multiple beams are oriented upward from a single RSD (either radar, lidar, or sodar), at a small angle from the vertical. In general, three or more beams are required to recover the full three-dimensional flow, but in the two-dimensional depiction shown here, two beams are sufficient to capture the vector wind flow. Also, the angle of the beams from the vertical has been exaggerated for illustration. The beams can only "see" the along-beam component of the flow. They are oriented at different angles to capture different vector components of the flow, from which the Cartesian vector components (horizontal and vertical wind) can be recovered through vector math. Ideally, the different vector components would always be measured at the same point in space, such

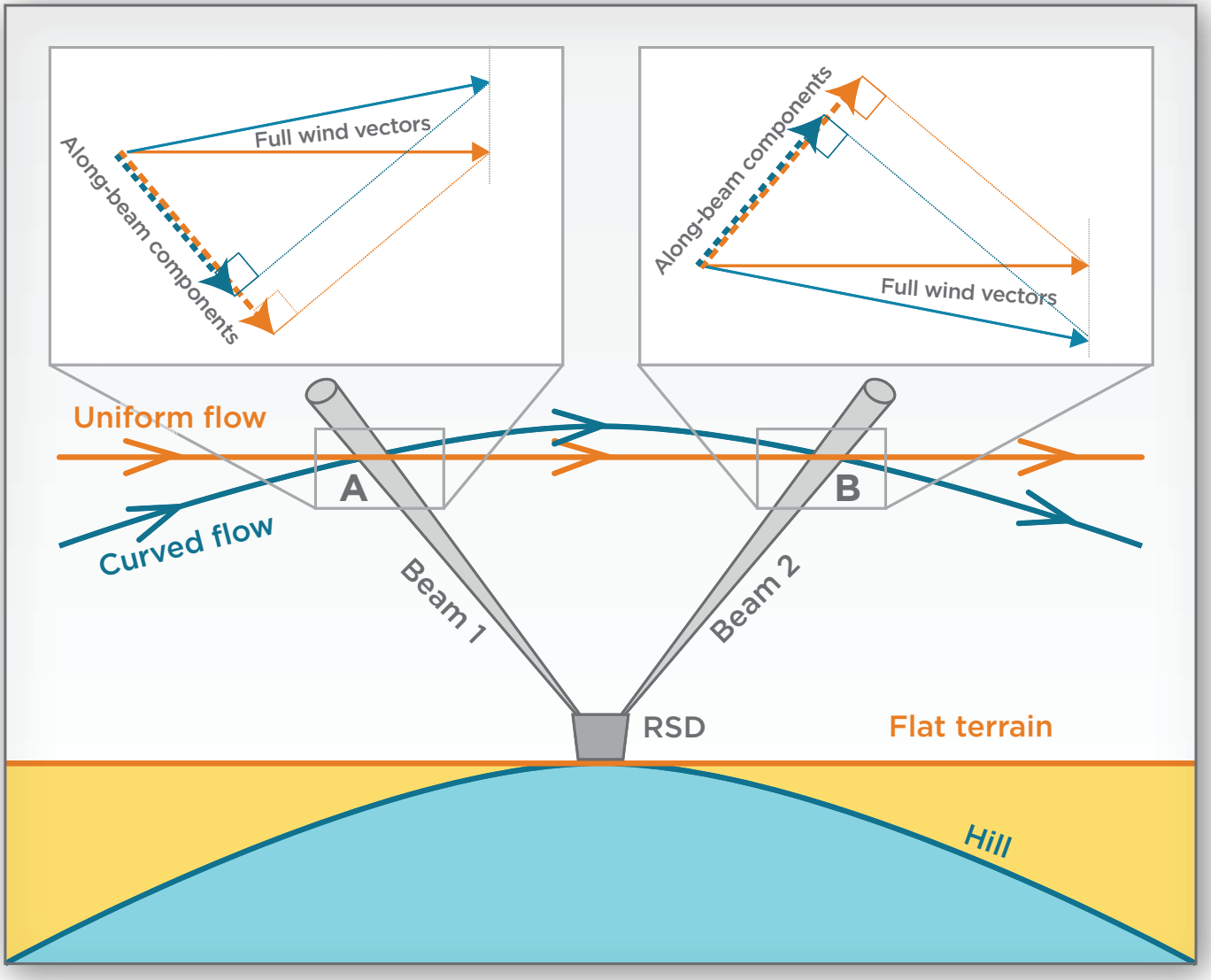

Figure 1. Schematic description of flow curvature bias.

as at a desired height directly above the RSD, but this does not occur with the divergent beam strategy. Instead, the two beams measure the wind at two different locations at the desired measurement height (points "A" and "B"), but they are treated as the same location in the retrieval math. In the flat terrain scenario, this does not matter because the flow is horizontally uniform, so the result is the same whether the different components are measured at the same horizontal location or separate horizontal locations. However, in the case of convex flow, on the upwind side, the beam crosses the flow slightly more perpendicularly than for the equivalent flat terrain flow, and it can be seen that the along-beam component toward the device is slightly smaller than for flat terrain. Meanwhile, on the downwind side, the same effect occurs, with the component away from the device again being smaller than in the flat terrain case. Because both components are biased low, the flow curvature perfectly imitates the effect of lower horizontal wind speed, resulting in a low bias in the retrieved wind speed.

Although not depicted here because it occurs less commonly, it can be shown that in a situation of concave flow (i.e., flow above a bowl or valley), the opposite effect occurs. Both the upwind and downwind beams are less perpendicular to the flow, resulting in larger along-beam components, and a positive bias in the retrieved horizontal wind speed. It is also important to point out that, if the terrain and associated flow are sloped but not curved (e.g., uniform upslope flow from left to right, not shown in diagram), the inbound component is reduced on the upwind side (as depicted), but the outbound component is increased on the downwind side (opposite to what is depicted), resulting in no bias after the vector math is carried out. In short, the flow is only biased when the inflow angle is different within the two beams. Uniform upslope or downslope flow can be measured by a RSD without bias.

The flow curvature bias can be approximated by the simple equation

$$B \approx -\frac{h}{R}\ , \tag{1}$$

where B is the bias (expressed as a decimal fraction or percent, with a value of zero indicating no bias), h is the measurement height above ground, and R is the radius of curvature of the flow (positive is convex or dome-shaped flow; negative is concave or bowl-shaped flow). Thus, the more sharply curved the flow, the larger in magnitude the bias; and for the same degree of curvature, the effect is stronger at higher heights. In fact, the dependence on h would suggest that the effect is, for example, four times stronger at 160 m than it is at 40 m. However, it should be noted that wind flow over complex terrain tends to flatten or smooth out with height, meaning that both R and h increase with height. Therefore, the ratio in equation (1) may slightly increase, decrease, or remain roughly constant with height, depending on the details of the terrain and flow dynamics.

2.2 CFD Simulations

Because RSDs can only measure the wind component along the beam path, the flow curvature cannot be determined from measurements of the device itself, no matter how many different beam angles are employed. Two general approaches have been studied to overcome this limitation. The first is to take additional measurements from other nearby locations, with beams that converge at the desired measurement point (a convergent beam strategy), rather than diverging from a single device. This can be accomplished either with multiple monostatic devices (i.e., devices that transmit pulses and receive their own returned backscatter); or a network of bistatic devices (i.e., a single transmitting device, surrounded by a cluster of devices that receive backscatter from the same point in space but from different directions). These approaches are complicated and require significant additional hardware and a larger measurement footprint, and are therefore not generally practical for wind industry use. The second approach is to use wind flow modeling to reproduce the full three-dimensional flow surrounding the RSD. Within that modeled flow, both the true wind vector directly above the device, and the divergent beam-recovered (biased) wind vector can be calculated. The model-predicted bias due to flow curvature is the beam-estimated speed minus the true speed, divided by the true speed (expressed as either a decimal fraction or a percent, with a value of zero indicating no bias). A correction factor can be calculated, as 1/(1+bias). This correction factor can be applied to the wind speeds measured by the RSD to remove the measurement bias due to flow curvature.

As the wind resource assessment community is well aware, all wind flow models have a degree of uncertainty, which might give one pause in using such models to make adjustments to wind speeds observed by RSDs. However, there are reasons to be optimistic about this approach. First, it is primarily the shape of the flow across the measurement cone that is important for estimating the bias; the magnitude of the flow is less important. Therefore, if the model captures the shape of the flow but is biased in magnitude, this will have little negative effect on the result. Second, the distance over which the model must simulate the flow curvature is very small. For example, Triton's beams are tilted 11.4 degrees from the vertical, so even at 200 m (the highest measurement height), the measurement cone is only 80 m across. It is not unreasonable to hope that wind flow models will have significant skill at reproducing the correct shape of the wind flow over such short distances. Ultimately, the ability of the model to perform the desired task can only be assessed with comprehensive validation, as is presented in this study.

Vaisala has partnered with WindSim to provide a rapidly configurable CFD model simulation for any specified location where a RSD is or might be deployed. The model uses a standardized grid to simulate the three-dimensional flow field over the RSD device, from which flow curvature bias (and correction factors) can be obtained in the manner described above. The WindSim CFD model has a long history of successful use in the wind energy industry for resource assessment, modeling of waked wind flow, and other applications. The characteristics of the WindSim simulations used in the present study are listed in Table 1. The simulation yields a gridded field of the three wind components (eastward, northward, and

Table 1. WindSim CFD model configuration

Domain	
Size of inner simulation domain	400 x 400 m
Grid spacing within inner simulation domain	5 m
Size of full domain	8000 x 8000 m
Coarsest grid spacing in outer domain	136 m
Vertical extent above highest elevation in domain	4500 m
Vertical grid spacing within lowest 200 m	20 m
Input datasets	
Input digital elevation models (and horizontal resolution)	NED (10m) in CONUS, ASTER (30m) at latitude > 60°, SRTM (90m) elsewhere
Input land use datasets models (and horizontal resolution in m)	NLCD (30m) in CONUS, CORINE (30m) in Europe, GLC30 (30m) elsewhere
Model details	
Height of boundary layer	500 m
Direction sectors simulated	16
Speed above boundary layer	10.0 ms^{-1}
Boundary condition at the top	Fixed pressure
Turbulence model	RNG k-epsilon
Stability	Neutral
Solver	General Collocated Velocity
Maximum iterations	800

upward) surrounding the RSD at the set of heights covering the measurement range of the device. Separate simulations are made for each of the sixteen standard wind sectors. After computing the vector math to extract the Doppler-retrieved and true horizontal wind speeds within the simulated wind flows, a look-up table is generated with flow curvature correction factors for each height and wind direction sector. The look-up table can be applied to an entire time series of remotely sensed measurements by interpolating the look-up table values to the desired height and precise direction measured by the RSD at each time point. It is noted that the direction itself can also be affected by terrain-induced flow inhomogeneities, but these are generally very small, typically only a few degrees at most, and so are ignored.

Finally, the comparison of winds measured by a RSD to a collocated met tower requires consideration of site calibration between the met tower and RSD. Tritons cannot be placed directly adjacent to a met tower, because fixed structures near a sodar can produce backscatter that contaminates the returned signal. Thus, Tritons are typically sited one to two tower heights away from the met tower. In complex terrain, this distance can be enough to yield a difference in the true wind speed between the RSD and the met tower. Fortuitously, the same CFD simulation that is used to estimate the flow curvature bias at the RSD can be configured to include the nearby met tower, and the simulated winds at the met tower can be output as well. The model-predicted site calibration bias is the simulated RSD-measured wind speed minus the simulated met tower wind speed, divided by the simulated met tower

wind speed (expressed as either a decimal fraction or a percent, with a value of zero indicating no bias). As for flow curvature, a correction factor can be calculated, as 1/(1+bias). This correction factor can be applied to the remotely sensed wind speed time series, to make the remotely sensed wind speeds comparable to the met tower wind speeds for validation. The correction factor can be applied either by itself or in conjunction with the flow curvature correction factor, as will be discussed further below.

3 Validation Study Design

3.1 *Dataset characteristics*

To test the CFD-based flow curvature correction, we gathered measurements from 26 Triton wind profilers with collocated met towers around the globe. Table 2 provides the global distribution of the sites chosen. Slightly over half the sites are in North America, with the remainder scattered throughout Europe, Africa, Asia, and Australia/Oceania. Table 2 also lists the sites by terrain type. These categories are subjectively assigned, but give a sense of the variety of terrain complexities included. We included a small number of flat sites, to check bias prediction accuracy where the effect is expected to be small. At 20 of the 26 sites, the Triton-met tower separation distance was less than 120 m. The remaining 6 sites had separation distances ranging from 120 to 370 m.

For each site, a period was chosen for comparison that had good data recovery and a variety of wind speeds and directions. The wind rose at most sites was not omnidirectional, so some direction sectors were underrepresented. For most of the Triton/met tower pairs, we were able to select a 3-month period of good simultaneous measurement. However, 4 pairs had only 2 months of simultaneous data, and 1 pair had only 1 month.

Table 2. Site counts by geographic region and terrain type

By region	Count
North America	14
South America	2
Europe	4
Africa	2
East Asia	1
Australia/Oceania	3

By terrain type	Count
Flat	4
Rolling	8
Hilly	6
Complex	8

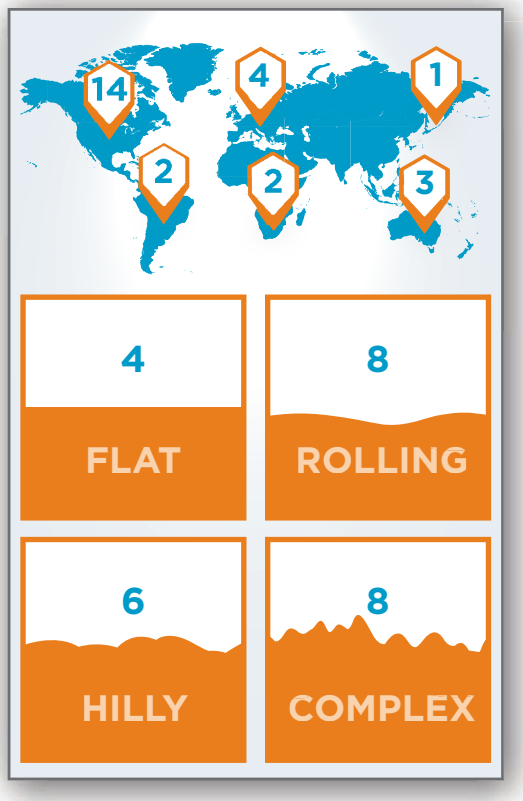

[1]In the case of redundant anemometers at the same height on a tower, the data were selectively averaged into a single time series (as described in Appendix A). Each redundant pair counts as a single anemometer in the total of 69.

The met towers were equipped with cup anemometers at heights ranging from 20 to 120 m, though only heights at or above 35 m were used in this study. In all, 69 anemometers were used[1], and the validation comparisons were performed at the anemometer heights, rather than at the Triton standard measurement heights.

3.2 *Data preparation*

Both the met tower and Triton data in each pair were quality controlled prior to inclusion in the validation analysis. Quality control procedures are described in Appendix A, including filtering procedures for both data sources, as well as procedures to ensure temporal alignment between the Triton and met tower data, and to interpolate Triton measurements to the met tower anemometer heights.

4 Validation study results

4.1 *The correction factors at individual sites*

To demonstrate if the CFD simulations capture the actual biases between the Triton and met tower, Figure 2 shows a few examples of the CFD-predicted biases versus wind direction, overlaid with the observed percent difference in mean wind speed between the uncorrected Triton and the collocated met tower. Each column in the plot depicts one of four sites chosen from the 26 sites in the study. The subset of sites shown here were selected because they have a more omnidirectional wind rose and therefore, more sectors to visually compare; and because they display a typical range of success of the CFD correction factors in capturing the observed wind speed differences. The two rows show the two different anemometer

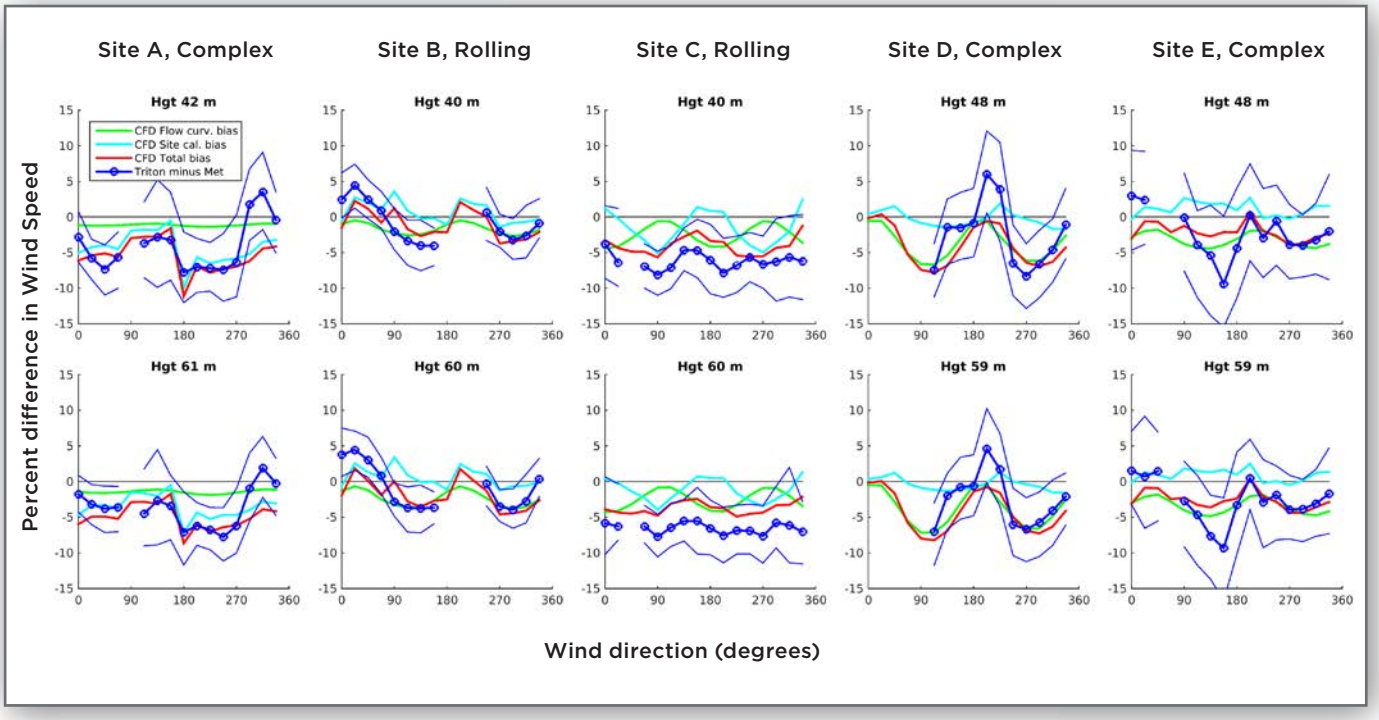

Figure 2. CFD model–predicted site calibration and flow curvature biases compared to observed differences (Triton-minus-met tower) at four sample sites. y-axis is observed percent difference in mean wind speed (or predicted bias), x-axis is wind direction sector. Each site had two anemometer heights for comparison (upper and lower rows).

heights that were available at each site. The CFD-predicted biases are shown in green (flow curvature bias) and cyan (site calibration bias). The combined bias, shown in red, is calculated by adding 1 to each bias, multiplying them, and subtracting 1. For biases that are a few percent in magnitude, this is approximately equal to the sum of the biases. The observed difference between the Triton and met tower mean wind speed by direction sector, expressed as a percent of the met tower mean wind speed, is shown in blue. For direction sectors in which there were less than 50 valid data points, the observed mean wind speed percent difference is not shown. The thin blue curves show the interquartile range of all the valid data points within each sector.

Examination of the CFD-predicted biases reveals a few interesting characteristics. The flow curvature bias is always negative in these four examples, reflective of hill or ridge-shaped terrain that produces convex flow curvature. This is generally the case across the dataset, with only a few exceptions (at sites not shown in this figure) where the terrain is slightly bowl shaped. The flow curvature bias also shows significant directional variability, often in the approximate shape of a sine wave, indicating flow (and underlying terrain) that has perpendicular axes of greater and lesser curvature, such as with an elongated hill. In contrast, the site calibration bias tends to vary around zero, with both positive and negative deviations in different direction sectors. Site calibration biases are typically smaller than flow curvature biases (Site A being an exception), and both vary with height.

The agreement between the predicted and observed biases by direction can be examined by comparing the red (predicted bias) curve and the blue (observed difference) curve. In most sectors/sites, the CFD-predicted bias is of the correct sign (red and blue curves on the same side of the zero line). In many sectors/sites, the agreement is quite good, where both the magnitude and directional pattern are well captured, but at other sectors/sites, there are significant differences (e.g., Site D, near 200 degrees; Site E, near 160 degrees). Site C shows good agreement in the directional pattern, but the entire predicted curve is offset from observed difference curve by ~4%. In general, the agreement is good, but the ultimate test is to apply the correction factors to the entire time series, and compare Triton mean wind speeds (corrected and uncorrected) to those measured by the towers.

4.2 *Validation results*

Performance of the CFD-based corrections across the full validation dataset is presented in the form of histograms (Figure 3) that show distributions across all 69 validation points of three metrics that compare the Triton and met tower-measured wind speeds: the coefficient of variation (R^2) of the 10-minute measurements; the root mean-squared (RMS) difference between the 10-minute measurements; and the percent mean wind speed difference. Results are shown for two validation experiments, one in which no corrections are applied, and one in which both the site calibration and flow curvature corrections are applied.

The histogram of 10-minute R^2 shows very little improvement after the corrections are applied. This is understandable, because the correction factors applied here are generally a few percent, and vary only with wind direction, which can often be steady for hours or

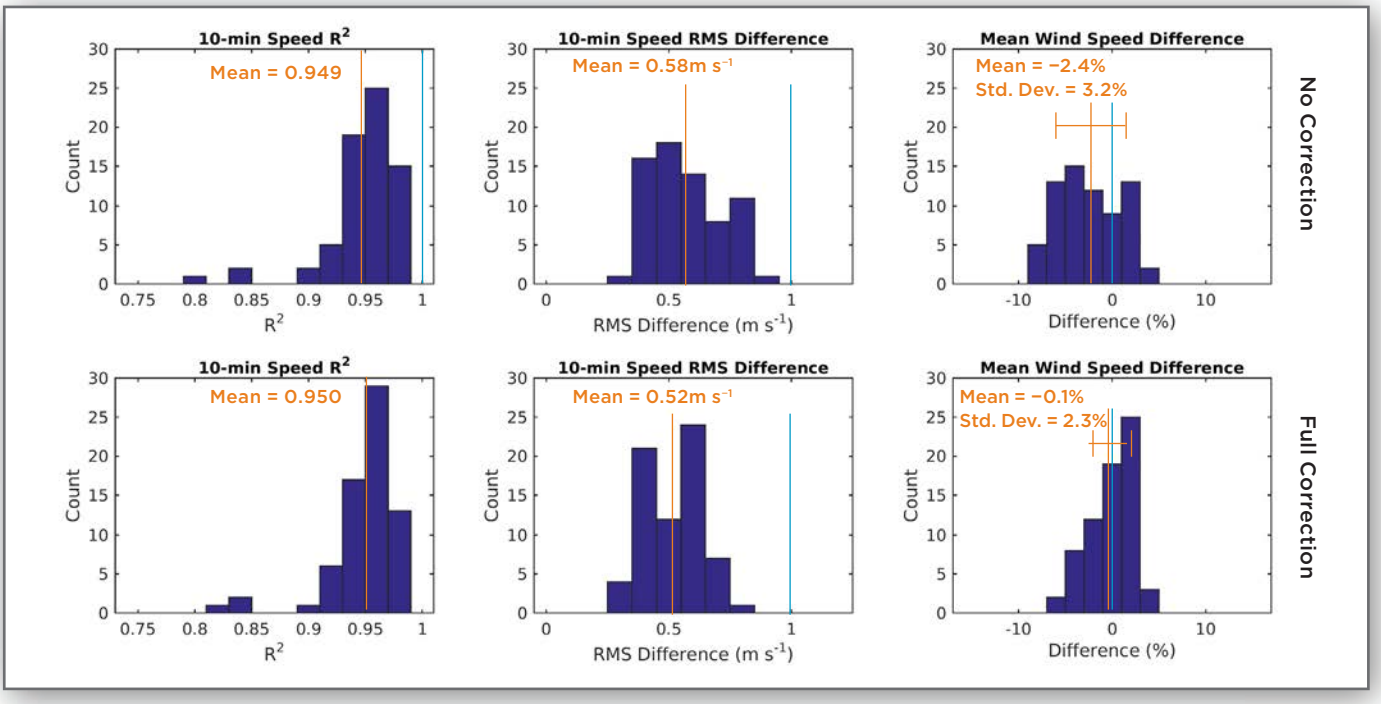

Figure 3. Histograms of 10-minute R^2, 10-minute RMS wind speed difference, and mean wind speed difference, for all 69 validation points. Top row shows "Control" experiment results, and bottom row shows "FullCorrection" results.

days at a time. Therefore, the correction factors are doing very little to improve short-term deviations between the Triton and met tower, which are what dominate the 10-minute R^2. The histogram of RMS difference of the 10-minute data shows somewhat more noticeable improvement. As with 10-minute R^2, it is affected by short-term deviations in wind speed, which the correction factors cannot reduce; but it is also affected by mean difference between the Triton and met tower, which the correction factors successfully reduce. That is seen even more clearly in the final histogram that shows the distribution of percent mean wind speed difference between the Triton and met tower. Prior to correction, the mean of percent mean wind speed difference across all 69 validation points was −2.4%, consistent with the expected predominance of convex flow curvature. The standard deviation of percent mean wind speed difference among the 69 validation points was 3.2%, indicating that varying amounts of flow curvature and/or site calibration bias were present in the uncorrected measurements. With the CFD-based corrections, the mean of percent mean wind speed difference was reduced to near zero (−0.1%), indicating a successful removal of the flow curvature and/or site calibration biases, at least in a dataset-wide average sense. The standard deviation of the percent mean wind speed difference that remained after correction is 2.3%. This is significantly lower than for the uncorrected measurements, but importantly, is still larger than the equivalent standard deviation from the flat-terrain validation study (1.3%). In other words, the CFD-based flow correction removes bias when averaged across all sites, but leaves a residual site-to-site uncertainty in mean wind speed, in addition to the uncertainty of purely flat-terrain measurements. Quantifying this uncertainty is the focus of the next section.

5 Uncertainty Analysis

5.1 *Partitioning of uncertainty among the known sources*

In addition to demonstrating that the CFD-based flow curvature correction performs well, this study aims to provide quantitative guidance on the remaining uncertainty of Triton's corrected wind speed, so that users of Tritons in complex terrain can assign uncertainty values to wind measurements. The first challenge in the uncertainty analysis is that the widths of the distributions of mean wind speed difference shown in the previous section include more than just Triton measurement uncertainty. Uncertainties in the tower measurements to which Triton is being compared, and in the site calibration correction derived from the CFD simulations, both contribute to the width of these distributions. However, neither of these uncertainties are relevant to the central question in using Triton data for wind resource assessment: What is the uncertainty in using Triton to measure the true mean wind speed at a location in complex terrain, after using the CFD-based flow curvature correction?

To help quantify the uncertainty we are interested in, we conducted four different validation experiments:

1. "NoCorr": The control, in which no correction factors are applied to Triton data.
2. "SiteCalOnly": Only the site calibration correction factors are applied to the Triton data.
3. "FloCurvOnly": Only the flow curvature correction factors are applied to the Triton data.
4. "FullCorr": Both site calibration and flow curvature correction factors are applied to the Triton data.

In each of these four experiments, the differences in mean wind speed between the Triton and met tower at the 69 tower validation points has a unique distribution, with a mean and standard deviation. The distributions for NoCorr and FullCorr are exactly those shown in the rightmost panels of Figure 3. Those for SiteCalOnly and FlowCurvOnly are not shown but were derived for the analysis.

In quantifying uncertainty, we are only concerned with the width of the distribution, and the standard deviation is used as the measure of width. Table 3 lists the standard deviations for the four experiments. The variances from the four experiments (which are the square of the standard deviation) can be partitioned into components representing different sources of uncertainty. The components are assumed to be statistically independent, so the total variance is the sum of component variances. The assumed sources of uncertainty for the four experiments are:

$$\sigma^2_{\text{T–M NoCorr}} = \sigma^2_{\text{SiteDiff}} + \sigma^2_{\text{FloCurvBias}} + \sigma^2_{\text{TriFlat}} + \sigma^2_{\text{Met}} \quad (2)$$

$$\sigma^2_{\text{T–M SiteCalOnly}} = \sigma^2_{\text{SiteCal}} + \sigma^2_{\text{FloCurvBias}} + \sigma^2_{\text{TriFlat}} + \sigma^2_{\text{Met}} \quad (3)$$

$$\sigma^2_{\text{T–M FlowCorr}} = \sigma^2_{\text{SiteDiff}} + \sigma^2_{\text{FloCurvCorr}} + \sigma^2_{\text{TriFlat}} + \sigma^2_{\text{Met}} \quad (4)$$

$$\sigma^2_{\text{T–M FullCorr}} = \sigma^2_{\text{SiteCal}} + \sigma^2_{\text{FloCurvCorr}} + \sigma^2_{\text{TriFlat}} + \sigma^2_{\text{Met}} \quad (5)$$

In the above equations, the total variances on the left side refer to the variances of the mean wind speed differences across the 69 validation points ("T–M" means "Triton minus Met"). In other words, these are the squared standard deviations for each experiment, whose values are listed in Table 3. The variances on the right-hand sides are as follows:

- "SiteDiff": the variance of differences in true mean wind speed at Triton and met tower locations, when no site calibration has been applied
- "FloCurvBias": the variance of the flow curvature biases with respect to true wind speed at the Triton locations, when no flow curvature correction has been applied
- "SiteCal": the remaining uncertainty in site differences after the (presumed imperfect) site calibration correction is applied
- "FloCurvCorr": the remaining uncertainty in flow curvature bias after the (presumed imperfect) flow curvature correction is applied
- "TriFlat": the uncertainty of mean wind speed measured by a Triton in flat terrain
- "TriMet": the uncertainty of mean wind speed measured by a met tower in flat terrain

Following the conclusions in the flat-terrain study, the last two variances are both assumed to be $(1\%)^2$.

What we are really interested in is isolating $\sigma^2_{\text{SiteCal}}$ and $\sigma^2_{\text{FloCurvCorr}}$. Note that none of the actual variances that we measured (the left-hand side terms) translates directly into either of these two quantities. However, by making some reasonable assumptions and manipulating equations (2)–(5) (see Appendix B), and using the values in Table 3 and the assumed value of $(1\%)^2$ for both $\sigma^2_{\text{TriFlat}}$ and σ^2_{Met}, we can estimate $\sigma^2_{\text{SiteCal}}$ and $\sigma^2_{\text{FloCurvCorr}}$ (as well as $\sigma^2_{\text{SiteDiff}}$ and $\sigma^2_{\text{FloCurvBias}}$, which we are less interested in). The resulting estimates of these four unknown quantities, expressed as percent standard deviations (square roots of the variances $\sigma^2_{\text{SiteDiff}}$, $\sigma^2_{\text{FloCurvBias}}$, $\sigma^2_{\text{SiteCal}}$, and $\sigma^2_{\text{FloCurvCorr}}$), are shown in Table 4. Across the entire dataset, the site calibration contributed an additional 0.8% uncertainty, and the flow curvature correction contributed an additional 1.8% uncertainty.

We now return to the central question of "What is the uncertainty in using Triton to measure the true mean wind speed at a location in complex terrain, after using the CFD-based flow curvature correction?". We define this desired uncertainty as $\sigma_{\text{TriCmplxCorr}}$, and it can be estimated by summing only the variances in equation (5) that affect the Triton uncertainty with respect

Table 3. Standard deviation (among all 69 validation points) of mean wind speed differences

Experiment	Standard Deviation of mean wind speed differences
NoCorr	3.2%
SiteCalOnly	3.2%
FloCurvOnly	2.6%
FullCorr	2.3%

Table 4. Individual uncertainty contributions to the overall standard deviation of mean wind speed differences.

Uncertainty Contribution	Value
$\sigma_{SiteDiff}$	1.2%
$\sigma_{FlowCurvBias}$	2.6%
$\sigma_{SiteCal}$	0.8%
$\sigma_{FlowCurvCorr}$	1.8%

to true wind speed, after flow curvature correction is applied: $\sigma^2_{TriCmplxCorr} = \sigma^2_{TriFlat} + \sigma^2_{FloCurvCorr}$. Taking the square root of this expression, we estimate $\sigma_{TriCmplxCorr} = 2.0\%$. This compares to the result inferred from the flat-terrain study, that the uncertainty of Triton mean wind speed with respect to truth over flat terrain is 1.0%.

5.2 *Site-specific uncertainty*

The uncertainties obtained above ($\sigma^2_{SiteCal}$, $\sigma^2_{FloCurvCorr}$, and $\sigma^2_{TriCmplxCorr}$) were derived from variances across the entire validation dataset. In other words, they are not site-specific. They are applicable to a site with terrain complexity similar to that of a typical site in the validation study. However, we seek a site-specific estimate of uncertainty for a Triton based on known parameters at a site. Such parameters might be derived from the terrain characteristics at the site, from the CFD simulation output, or from the Triton measurements themselves. They should not be dependent on collocated met tower measurements, because Tritons are not always deployed with a collocated met tower.

There are several challenges to identifying good parameters for estimating site-specific uncertainties. Not only is the dataset small, but the target variable is a variance, so each data point of variance requires several individual validation data points. Additionally, we do not have direct observations of the errors associated with the desired individual contributions to uncertainty represented by the right-hand side terms in equation (5). We only have observations of the percent difference in mean wind speed between the Tritons and collocated met towers, i.e., the differences whose variance is $\sigma^2_{T-MFullCorr}$, which is the left-hand side of equation (5). Therefore, we must seek relationships between our candidate parameters and $\sigma^2_{T-M\ FullCorr}$, and then partition the site-specific prediction of $\sigma^2_{T-MFullCorr}$ among the various contributions on the right-hand side of equation (5) in a reasonable way. With these caveats, we proceed cautiously to explore whether useful predictors of site-specific uncertainty can be found.

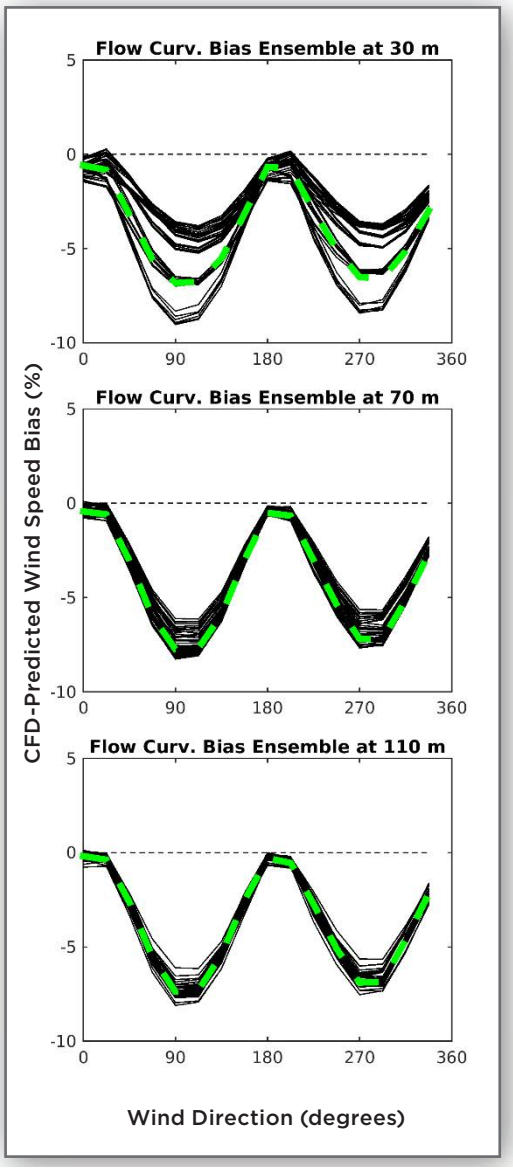

Figure 4. 42-member ensembles of CFD-predicted flow curvature bias versus wind direction, at three different heights at Site D.

We considered the following three candidate parameters that might be related to $\sigma^2_{T-MFullCorr}$:

1. The magnitude of the site calibration correction.
2. The height above ground of the measurement point.
3. The ensemble spread of site calibration correction.

Parameter #1 is included based on a common assumption that the uncertainty of a parameter is proportional to the magnitude of that parameter. To distill the sectorized correction factors down to a single number, we take the absolute value of the average of the applied correction during the entire time period of the validation comparison. Parameter #2, height above ground, was included because we observed that correction factors varied more smoothly and sinusoidally with direction sector at higher heights than at lower heights. Therefore, we hypothesized that the correction factors might be more certain at higher heights.

The ensemble spread parameter (#3) requires additional explanation. In our testing of the CFD-based flow corrections, we tried calculating the biases from the CFD model output in slightly different ways, e.g., using beam orientations or zenith angles that were slightly different from the actual values for Triton, or moving the Triton position slightly within the model simulated wind field grid. We found that at some sites, the resulting model-predicted site calibration or flow curvature biases were very sensitive to these small differences in the calculation method, whereas at other sites, they were insensitive. We hypothesized that the uncertainty of the bias estimates might be larger at more sensitive sites, for several reasons:

- There is some uncertainty in the exact position of the Triton.
- There is some uncertainty in the exact orientation of the Triton beams

- The input terrain and land use datasets for the CFD model are imperfect and have finite resolution.
- It is probably more challenging for the CFD model to accurately simulate the flows that result in the greater sensitivity.

To define a parameter that quantifies this sensitivity, we produced ensembles of correction factors at each site, by moving the Triton to six locations that are 20 m away from the actual location and evenly distributed in direction from the actual location; by rotating the beam configuration by 180°; and by using three different beam azimuth angles (5.7°, 11.4°, and 17.1°, where 11.4° is the actual zenith angle used by Triton). This yielded 42 ensemble members (7 locations times 2 beam orientations times 3 zenith angles). An example of the ensemble of flow curvature biases for Site D is shown in Figure 4. To arrive at a single parameter expressing "ensemble spread" for a particular site, we applied the ensemble of correction factors to the Triton wind time series, calculated the time-averaged correction factor of each ensemble member, and expressed the ensemble spread as the percent standard deviation of those time-averaged corrections at the site.

Figure 5 illustrates the strength of the relationships of the 3 candidate parameters to the squared differences in mean wind speed. Each panel shows a scatter plot of the squared percent mean wind speed difference between Triton and met tower from the 69 validation points (*y*-axis), versus one of the three parameters being tested (*x*-axis). If there is a relationship between *x* and the variance of mean wind speed difference, one should see a larger vertical spread of the points as one moves toward either positive or negative *x*. This is difficult to visualize considering the different densities of points within difference ranges of *x*. To help, the data were subdivided into quintiles of x. Each red point shows the quintile-average of *x*, versus the mean of *y* within the quintile of x (which is an estimate of $\sigma^2_{\text{T–MFullCorr}}$ for that quintile of *x*). With the quintile values shown, a relationship would express itself as a positive or negative trend in the red points. Best-fit lines and R^2 are shown, to further illustrate the relationship.

The first panel (Figure 5a) shows the relationship between the squared mean wind speed differences and the first candidate parameter, the absolute value of time-mean flow curvature correction. Contrary to our hypothesis, there is only a weak positive, poorly correlated trend in the red points. Therefore, the magnitude of the flow curvature correction factor is not a useful predictor of uncertainty. We note here that, although not listed above as one of the candidate parameters, we similarly tested the magnitude of the time-mean site calibration correction factor, but the relationship of $\sigma^2_{\text{T–M FullCorr}}$ to this parameter was similarly erratic and poor.

The scatter plot of squared mean wind speed differences versus height (Figure 5b) suggests an inverse relationship of $\sigma^2_{\text{T–MFullCorr}}$ to height (red dots, line). It is encouraging to see that corrected wind speeds are more certain at higher heights, especially since the industry trend is toward use of higher and higher hub heights. However, the use of height alone as a predictor of uncertainty is unsatisfying because it carries no site-specific information.

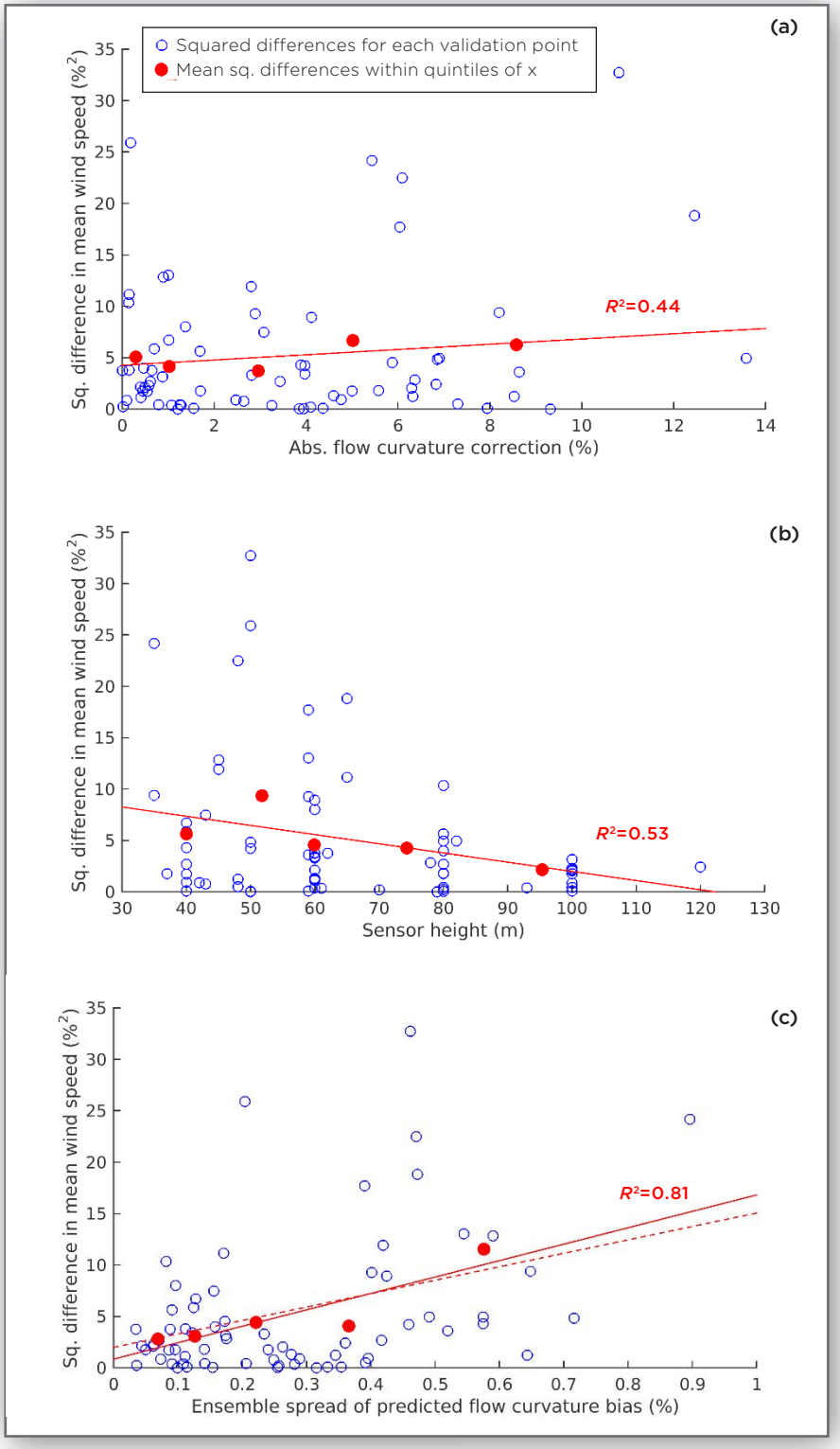

Figure 5. Scatter plots of squared percent differences of mean wind speed between the Triton and met tower (y) vs. various parameters (indicated on each x axis) at the 69 validation points. Red dots are averages of x and y values within quintiles of x. Red lines are best-fit line to the red dots, with coefficient of variation (R^2) shown. In (c), the dashed red line is the best fit line forced to pass through the y-intercept of 2.0.

Finally, the scatter plot for candidate parameter #3, ensemble spread of flow curvature correction (Figure 5c), shows a strong positive relationship between this parameter and $\sigma^2_{T-MFullCorr}$ (red dots and line, $R^2 = 0.81$). An additional benefit of the ensemble spread parameter is that it generally decreases with height, as can be seen from the clusters of curves in Figure 4. It therefore includes some of the inverse relationship between uncertainty and height that was seen in Figure 5b, in addition to a site-specific component of the relationship. Note, we also calculated an ensemble spread for the site calibration correction following the same procedure as for flow curvature correction. We determined, however, that the two ensemble spreads (for site calibration and flow curvature correction) did not provide independent information, as they were strongly correlated with each other ($R^2 = 0.70$). Considering the positive aspects of the flow curvature ensemble spread discussed above, and the fact that the site calibration correction would not always be available because there is not always a collocated met tower, we pursued using only the flow curvature ensemble spread to estimate site-specific uncertainty.

The equation of the best-fit line in Figure 5c can be expressed as

$$\sigma^2_{T-MFullCorr,Site} = mE+b, \quad (6)$$

where $\sigma^2_{T-M\ FullCorr,Site}$ is the site-specific value of $\sigma^2_{T-M\ FullCorr}$, E is the ensemble spread, and m and b are the regression slope and intercept. The linear fit yielded a minimum $\sigma^2_{T-MFullCorr,Site}$ at x = 0 of 1.0%², but it should not be lower than the flat-terrain value of $\sigma^2_{T-MFullCorr} = \sigma^2_{TriFlat} + \sigma^2_{Met}$ = 2.0%², so we recalculated the linear fit, forcing it to pass through the y-intercept of 2.0. This slightly adjusted line is shown as a dashed red line in Figure 5c, and this is the linear fit that is used. What remains is to partition the term mE between the site-specific estimates of the site calibration and flow curvature correction uncertainties, $\sigma^2_{SiteCal}$ and $\sigma^2_{FloCurvCorr}$. To do that, we assume that the ratio of the magnitudes of these two site-specific uncertainties is the same as the ratio of the magnitudes of means of these two uncertainties across the entire dataset, which are known (the last two entries in Table 4). This leads to the site-specific version of equation (5):

$$\sigma^2_{T-MFullCorr,Site} = \sigma^2_{SiteCal,Site} + \sigma^2_{FloCurvCorr,Site} + \sigma^2_{TriFlat} + \sigma^2_{Met} \quad (7a)$$

$$= \frac{\sigma^2_{SiteCal}}{\sigma^2_{SiteCal} + \sigma^2_{FloCurvCorr}} mE + \frac{\sigma^2_{FloCurvCorr}}{\sigma^2_{SiteCal} + \sigma^2_{FloCurvCorr}} mE + \sigma^2_{TriFlat} + \sigma^2_{Met} \quad (7b)$$

To test this equation, we calculated three different site-specific uncertainties for each of the 69 sensor validation points in the dataset:

1. $\sigma^2_{FloCurvCorr,Site}$, the uncertainty of the mean wind speed measured by Triton, due only to the flow curvature correction. This is square root of the second term on the right-hand side of equation (7a,b).

2. $\sigma^2_{TriCmplxCorr,Site}$, the uncertainty of the mean wind speed measured by Triton with respect to true wind speed, after flow curvature correction is applied. This is the square root of the second and third terms on the right-hand side of equation (7a,b)

$$\sqrt{\sigma^2_{FloCurvCorr,Site} + \sigma^2_{TriFlat}}$$

3. $\sigma^2_{T-MFullCorr,Site}$, the uncertainty of the difference between mean wind speeds measured by Triton and met tower, after site calibration and flow curvature corrections are applied. This is the square root of the full uncertainty defined in equation (7a,b).

The ranges of these uncertainties (minimum, median, and maximum) are shown in Table 5. The middle row, $\sigma^2_{TriCmplxCorr,Site}$ (and number 2 above), is most relevant to wind resource assessment. The minimum, 1.2%, is close to the uncertainty deduced from the flat-terrain validation study. The highest value is 3.3%, still low enough to provide valuable additional information in a project wind resource assessment and reduce the total uncertainty on the project's energy estimate. Finally, Table 6 shows the mean predicted uncertainty for two different groupings of the 69 validation points. The first is by type of terrain. As expected, more complex terrain types are characterized by greater uncertainty. The second grouping is by terciles of sensor height. The predicted uncertainty reduces as height is increased, consistent with the reduction with height of the ensemble spread parameter, which is used to estimate the uncertainty.

Table 5. Minimum, median, and maximum predicted site-specific uncertainties, among all 69 validation points in study.

Type of Uncertainty	Min	Median	Max
Additional uncertainty of Triton mean wind speed due solely to flow curvature correction	0.6%	1.6%	3.1%
Total uncertainty of Triton mean wind speed (relative to truth), after flow curvature correction	1.2%	1.9%	3.3%
Total uncertainty of Triton minus met tower mean wind speed, after site calibration and flow curvature correction	1.6%	2.3%	3.7%

Table 6. Mean predicted site-specific uncertainties of Triton mean wind speed (relative to truth) of the 69 validation points in the study, grouped by terrain type, and by height terciles..

Type of Terrain	Uncertainty
Flat	1.3%
Rolling	1.9%
Hilly	2.2%
Complex	2.2%
By Height Tercile	**Uncertainty**
Low (mean height = 43 m)	2.2%
Medium (mean height = 60 m)	1.9%
High (mean height = 89 m)	1.6%

6 Conclusions

Vaisala has partnered with WindSim to develop a CFD model–based correction to flow curvature bias incurred by remote sensing devices when used in complex terrain. Using a validation dataset comprised of 26 customer-supplied Triton wind profilers collocated with met towers at sites across the globe in varying degrees of terrain complexity, this study has demonstrated the following:

- The CFD-based simulations largely capture the differences that are seen between the Triton and met tower-measured mean wind speeds, by direction sector and height.
- Application of the CFD correction factors reduces the dataset-wide difference in mean wind speed measured by Triton and met towers from −2.4% to −0.1%. In other words, the dataset-wide bias is removed by the CFD-based corrections.
- Although the dataset-wide Triton bias is removed by the flow curvature correction, the correction leaves a residual uncertainty, over and above the uncertainty associated with Triton measurements in flat terrain. The remaining uncertainty in the difference between Triton and met tower mean wind speeds is 2.3%, compared to 1.3% in Vaisala's 2015 validation study of Triton in flat terrain.
- By performing multiple experiments and isolating the different contributions to the uncertainty of Triton measurement with respect to the met tower, we showed that the remaining uncertainty in the Triton measurements with respect to true wind speed is 2.0% after the flow curvature correction is applied. This result can be compared to the 1.0% uncertainty found in the flat-terrain study.
- We developed an ensemble of flow curvature bias estimates by perturbing the calculation method, and found the ensemble spread to be a good predictor of site-specific uncertainty of the corrected Triton measurements with respect to true wind speed. Using this approach, we found that the uncertainty of Triton mean wind speed ranges from 1.2% at the least uncertain validation point, to 3.3% at the most uncertain validation point, with a median uncertainty of 1.9%.
- The uncertainty tends to decrease with measurement height, which is an encouraging result considering the ever-increasing heights of modern wind turbines.

In summary, this study clearly demonstrates the value of correcting remotely sensed winds in complex terrain with CFD-based flow curvature correction. Moreover, this study is built on validation of customer deployed Tritons in real-world conditions at diverse locations across the globe. This is the same approach used in the previous flat-terrain validation study, and it is the position of Vaisala and WindSim that this method is the best way to develop meaningful uncertainty estimates for remote sensing in real-world situations.

Appendix A Data quality control and alignment

Both the met tower and Triton data in each pair were quality controlled (QC'd) prior to inclusion in the validation analysis. The met tower data were reviewed for the following issues, and appropriate filters or adjustments were made:

- The functions to convert anemometer output to wind speed, if provided, were inspected for reasonableness.
- Data recorded by malfunctioning anemometers were excluded.
- Anemometer data affected by the tower or surrounding structures were excluded.
- Periods of anemometer dragging were excluded.
- Periods of icing that affect the accuracy of wind speed and direction measurements were excluded.
- Sectors that were potentially waked by nearby turbines were excluded.
- Redundant anemometers at the same height were selectively averaged, meaning that at each time point, if both anemometers provided a value that met the above QC criteria, their average was used; if only one anemometer provided a QC'd value, its value was used; and if neither provided a QC'd value, the value was set to missing.

For the Triton data, time points were set to missing for the following conditions[2]:

- Quality factor[3] < 98
- Absolute value of vertical velocity > 1.0 m s^{-1}
- Wind speed < 4.0 m s-1 or > 16.0 m s^{-1}

Simultaneity of the Triton and met tower data was assured by examining lag correlation plots. Triton data were interpolated in the vertical to the met tower anemometer heights for proper comparison, by using power-law interpolation between the nearest bracketing standard Triton measurement heights.

Finally, a "many-outlier test" [3] was employed, based on the distribution of 10-minute differences between the Triton and met tower-measured wind speeds. This test resulted in rejection of 0.5% of the time points that remained in the entire dataset after all of the above met tower and Triton filters were applied.

[2]Note that both the quality factor and vertical velocity thresholds are more restrictive than Vaisala's normally recommended thresholds (90 and 1.5 m s^{-1}, respectively). These more restrictive values were chosen because in this study, we are less concerned with maximizing data recovery, and more concerned with including only high-quality data, so that the effect of terrain-induced flow curvature can be isolated as much as possible.

[2]The Triton quality factor is a quantity ranging from 0–100, reported at every height and 10-minute time point, that indicates the confidence in the accompanying speed and direction measurements at that height and time point. It is described in more detail in a document available from Vaisala [4].

Appendix B Derivation of partitioning of uncertainty contributions

To simplify equations (2)–(5), we make the following definitions:

$$A = \sigma^2_{\text{T-MNoCorr}} - \left(\sigma^2_{\text{TriFlat}} + \sigma^2_{\text{Met}}\right), \quad (8)$$

$$B = \sigma^2_{\text{T-MSiteCalOnly}} - \left(\sigma^2_{\text{TriFlat}} + \sigma^2_{\text{Met}}\right), \quad (9)$$

$$C = \sigma^2_{\text{T-MFloCurvOnly}} - \left(\sigma^2_{\text{TriFlat}} + \sigma^2_{\text{Met}}\right), \text{ and} \quad (10)$$

$$D = \sigma^2_{\text{T-MFullCorr}} - \left(\sigma^2_{\text{TriFlat}} + \sigma^2_{\text{Met}}\right). \quad (11)$$

Substituting these into equations (2)–(5) yields:

$$A = \sigma^2_{\text{SiteDiff}} + \sigma^2_{\text{FloCurvBias}} \quad (12)$$

$$B = \sigma^2_{\text{SiteCal}} + \sigma^2_{\text{FloCurvBias}} \quad (13)$$

$$C = \sigma^2_{\text{SiteDiff}} + \sigma^2_{\text{FloCurvCorr}} \quad (14)$$

$$D = \sigma^2_{\text{SiteCal}} + \sigma^2_{\text{FloCurvCorr}} \quad (15)$$

The terms *A, B, C,* and *D* include measured or assumed values, so they are known. The variances on the right-hand sides are unknown. Although there are four equations in four unknowns, the system does not yield a unique solution. Therefore, we make an additional assumption, that for each physical phenomenon that is corrected with the CFD simulation (site calibration and flow curvature bias), the ratio of the remaining uncertainty (after the correction) to the original uncertainty (before the correction) is the same for both phenomena, and is defined as *R*:

$$R = \frac{\sigma^2_{\text{SiteCal}}}{\sigma^2_{\text{SiteDiff}}} = \frac{\sigma^2_{\text{FloCurvCorr}}}{\sigma^2_{\text{FloCurvBias}}} \quad (16)$$

Substituting, equations (12)–(15) become:

$$A = \sigma^2_{\text{SiteDiff}} + \sigma^2_{\text{FloCurvBias}} \quad (17)$$

$$B = R\sigma^2_{\text{SiteCal}} + \sigma^2_{\text{FloCurvBias}} \quad (18)$$

$$C = \sigma^2_{\text{SiteDiff}} + R\sigma^2_{\text{FloCurvCorr}} \quad (19)$$

$$D = R\sigma^2_{\text{SiteCal}} + R\sigma^2_{\text{FloCurvCorr}} \quad (20)$$

This system is now over-specified. Adding equations (17) and (20), and also equations (18) and (19), yields a required sum, $A+D=B+C$. However, the actual values of *A, B, C,* and *D,* which we will designate with subscript "1", will not exactly agree with this required sum. If

the "ratio assumption" described above is good, they will be close, but we want to proceed with a set of values of *A, B, C,* and *D* that exactly agree with the required sum, so we define an offset, ε, to produce such a set of values. The adjusted values, which are unsubscripted to indicate that they satisfy the required sum, are defined as $A=A_1+\varepsilon$, $D=D_1+\varepsilon$, $B=B_1+\varepsilon$, and $C=C_1+\varepsilon$. Substituting these into the required sum yields an expression to calculate ε:

$$\varepsilon = (B_1 + C_1 - A_1 - D_1)/4 \,. \tag{21}$$

The resulting value of ε is 0.4, in "squared percent" (consistent with a variance). Table 7 shows the actual values of *A, B, C,* and *D* as obtained from the mean wind speed difference variances, as well as the values adjusted to satisfy the required sum (also in squared percent). These numbers suggest that the adjustment is small compared to the values of *A, B, C,* and *D*, indicating that the "ratio assumption" is reasonably valid.

Table 7. Actual and adjusted values of A, B, C, and D constants.

Quantity	Actual value (in percent squared)	Adjusted value (in percent squared)
A	8.0	8.4
B	8.0	7.6
C	5.0	4.5
D	3.3	3.7

Division of equation (20) by (17) (or alternatively, the sum of (18) and (19) divided by (17)) yields two equivalent expressions for the assumed ratio, *R*:

$$R = D/A, \text{ or } R = (B + C - A)/A \,. \tag{22}$$

Using the adjusted values for *A, B, C,* and *D*, equation (16) yields $R = 0.44$, indicating that the remaining uncertainty (as a variance) after either site calibration or flow curvature correction is performed is 44% of the uncertainty associated with each of those phenomena if they are not corrected.

Subtraction of equations (17) and (18), as well as (17) and (19), yields expressions for the four unknown variances:

$$\sigma_{\text{SiteDiff}} = (A - B)/(1 - R) \tag{23}$$

$$\sigma_{\text{FloCurvBias}} = (A - C)/(1 - R) \tag{24}$$

$$\sigma_{\text{SiteCal}} = R(A - B)/(1 - R) \tag{25}$$

$$\sigma_{\text{FloCurvCorr}} = R(A - C)/(1 - R) \tag{26}$$

The values of these uncertainties, expressed as standard deviations (square root of variances) are the values shown in Table 4.

References

[1] Vaisala, 2015: Triton remote sensing systems: Comparing accuracy with collocated met towers. Vaisala white paper, 19 pp. Available from vaisala.com/energy.

[2] Bradley, S., A. Strehz, and S. Emeis, 2015: Remote sensing winds in complex terrain: a review. *Met. Z.,* 24, 547-555.

[3] Rosner, B., 1983: Percentage points for a generalized ESD many outlier procedure. *Technometrics,* 25, 165-172.

[4] Vaisala, 2014: Wind data processing made easy: Using Triton's quality factor. Vaisala white paper, 7 pp. Available from vaisala.com/energy.

Ref. B211724EN-A